

FROM THE DEPARTMENTS OF RADIATION PHYSICS, UNIVERSITY OF GOTHENBURG, S-413 45 GOTHENBURG,
AND UNIVERSITY OF UMEÅ, S-901 85 UMEÅ, SWEDEN.

LIQUID IONIZATION CHAMBER FOR ABSORBED DOSE DETERMINATIONS IN PHOTON AND ELECTRON BEAMS

K.-A. JOHANSSON and H. SVENSSON

Several investigations of the properties of the liquid ionization chamber have been carried out (MATHIEU 1968, WICKMAN 1974, CASANOVAS 1975, CHU et coll. 1980). Several advantageous features, as compared with the conventional ionization chamber, have also been pointed out. In spite of this, the chamber has not come into general use, mainly because of practical problems. A practical liquid ionization chamber, which is a further development of the plane-parallel liquid ionization chamber designed by WICKMAN, has been routinely used for several years. The practical experiences are now reported and important characteristics shown, e.g. energy dependence and recombination losses. In addition some fundamental physical properties such as the mean energy expended in the liquid per ion pair formed and the initial recombination losses have also been analysed.

Chamber design and performance

The construction of the liquid ionization chamber is shown in Fig. 1. The chamber has a very small sensitive volume (2.4 mm^3) and therefore a good spatial resolution. The exterior dimensions of the chamber are equivalent to the NACP plane-parallel air ionization chamber (cf. MATTSSON et coll. 1981) for measurements in electron beams. The chamber is of the plane-parallel type with a guard. The conducting layer is of beryllium, which has been evaporated onto styrene-copolymer (Rexolite) walls. The liquid used for this chamber is 2,2,4-trimethylpen-

tane (Merck: Isooctan für die Spektroskopie). The sensitive liquid layer is very thin ($0.32 \pm 0.03 \text{ mm}$) in order to assure a high electric field strength over the layer and to give short travel distances for the ions. The diameter of the sensitive layer is $3.1 \pm 0.05 \text{ mm}$. The density of the liquid, ρ , is $0.69 \text{ g} \cdot \text{cm}^{-3}$.

The liquid in the chamber evaporates slowly from the chamber and after about a month so much liquid may have disappeared from the cavity that the liquid has to be refilled. The response of the chamber will change if an air bubble will come into the sensitive liquid layer (i.e. in front of the collecting electrode). An accumulated absorbed dose of several kGy may also change the response of the chamber with a few per cent (WICKMAN) and the liquid has to be changed. Therefore an equipment has been produced, suitable to refill the liquid into the chamber (Fig. 2). In order to carry out a refilling, the chamber is taken into a vacuum container and the used liquid is pumped out. When this liquid has left the chamber, the liquid ampoule is connected to the chamber and the vacuum pump is again started. When air bubbles appear in the ampoule the air-inlet valve is again opened and the chamber cavity is filled with liquid. Any air remaining in the cavity is efficiently removed by repeated pumping and opening of the air-inlet valve. The whole procedure takes about 10 min.

Stability and leakage. The liquid ionization chamber has been used as a dosimeter at an electric field

Accepted for publication 30 August 1982.

strength of about $2.7 \text{ kV} \cdot \text{mm}^{-1}$. It appears from Fig. 3 that the voltage must be constant within $\pm 3 \text{ V}$ in order to attain a precision within $\pm 0.1\%$ (i.e. $0.03\% \cdot \text{V}^{-1}$). The reproducibility and the long-time stability of three chambers have been determined from measurements carried out during several months in a ^{60}Co γ -beam at fixed geometry. Temperature corrections have been applied. The standard deviation of the individual measurements for each of the chambers was 0.7, 0.9 and 0.9 per cent. The chambers were refilled several times during these tests. No significant change of the response (charge/absorbed dose) was observed after a refill. The response was also insensitive to the absorbed dose already given to the liquid at least up to about 1 kGy as some of the chambers had received this absorbed dose before refilling. WICKMAN found that the response was reduced by about 1 per cent when the accumulated absorbed dose to the liquid was 1 kGy.

The leakage current of an irradiated chamber increases with the electrode potential difference and the temperature (WICKMAN). However, the leakage generally turns out to be constant during a series of measurements under normal temperature variations. The potential on the chamber has to be chosen low enough so that this leakage is small but high enough so that the general recombination is acceptable. A good compromise for this chamber for dose rates used in therapy, i.e. 0.1 to $3 \text{ Gy} \cdot \text{min}^{-1}$, is about $3 \text{ kV} \cdot \text{mm}^{-1}$. The leakage current for all the different chambers was between 0.1 and 1 pA (~ 0.4 – $4 \text{ nGy} \cdot \text{min}^{-1}$). Leakage values larger than a few pA indicate that the liquid should be changed. When the dose rate is low the time for each irradiation, or the integrating-time of the electrometer must be registered in order to allow calculation of the 'net-collected' charge.

Temperature dependence. The mobility of the ions in the liquid increases when the temperature of the liquid increases and the initial recombination will therefore decrease as more ions can be collected at a given chamber potential. The response of the chamber increases almost linearly with the temperature for a fixed chamber potential. The magnitude of the temperature correction factor depends on the electric field strength. For a high electric field a large fraction of the ions produced along the track are collected and a change in the mobility caused by the temperature will have a relatively small effect on the response. The experimentally obtained tempera-

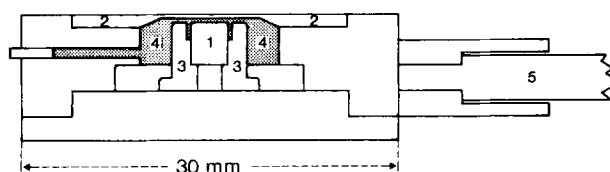


Fig. 1. Diagram of the plane-parallel liquid ionization chamber. 1) Collecting electrode. 2) Front window with high tension electrode. 3) Guard electrode. 4) The liquid 2,2,4-trimethylpentane. 5) Triaxial cable. The guard, the collecting electrode and the front window are covered with a thin evaporated layer of beryllium.

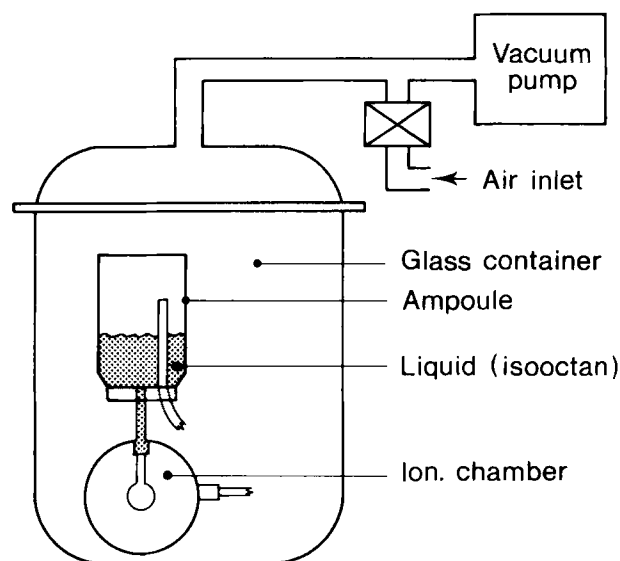


Fig. 2. The equipment for refilling of the chamber.

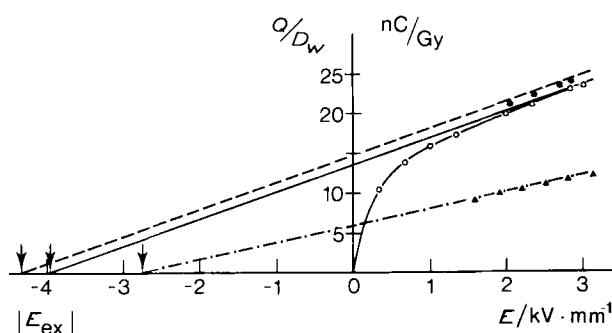


Fig. 3. The measured ionization charge, Q , divided by the absorbed dose to water, D_w , versus the electric field strength, E , for different radiation qualities. $|E_{\text{ex}}|$ is the extrapolated field strength. The extrapolated lines have been corrected for the general recombination losses. Experimental results are given for electron beam with $\bar{E}_0 = 11 \text{ MeV}$ (\bullet), for ^{60}Co γ beam (\circ) and for 200 kV roentgen ray with $\text{HVL} = 1.1 \text{ mm Cu}$ (\blacktriangle).

ture correction factor, t_{corr} , to be applied to the measured charge Q is

$$t_{\text{corr}} = 1 - (t - t_{\text{ref}})k \quad (1)$$

where t = the temperature of the liquid, in $^{\circ}\text{C}$, and

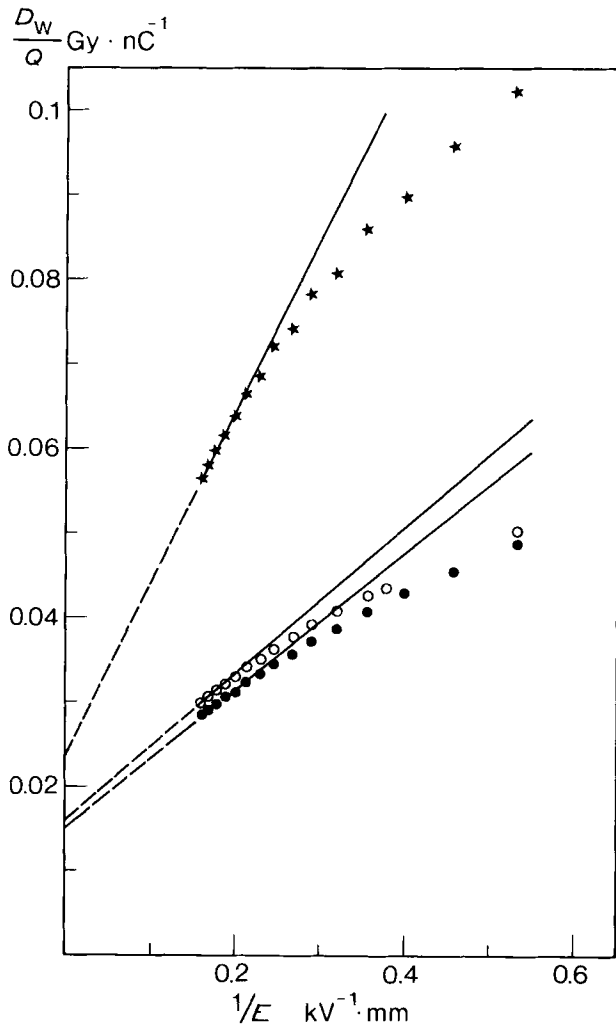


Fig. 4. Plots of the inverse of the ionization charge, Q , multiplied by the absorbed dose to water, D_w , against the inverse of the electric field strength, E , for different radiation qualities. The figure is a so-called Jaffe plot. Experimental results are given for 200 kV roentgen ray (*), for ^{60}Co γ beam (\circ) and for electron beam with $E_0=11 \text{ MeV}$ (\bullet).

Table 1

The electric field strength dependent factor, k , used in equation 1 for calculation of the temperature correction factor, t_{corr}

Field strength. ($\text{kV} \cdot \text{mm}^{-1}$)	$k \text{ (}^\circ\text{C)}^{-1}$		
	Present investigation	WICKMAN (1974)	CASANOVAS (1975)
15	0.0046		0.0035
27	0.0040 ± 0.0002	0.003	0.003
47	0.0033		

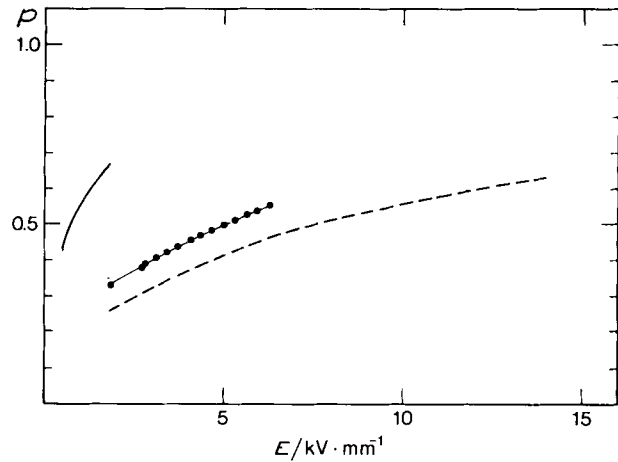


Fig. 5. The ion escape probability, p , versus the electric field strength, E , for ^{60}Co γ beams. The curves are determined from a so-called Jaffe plot. The solid line is from Chu et coll. (1980) with extrapolation from 0.8 to 1.6 $\text{kV} \cdot \text{mm}^{-1}$, the broken line is from Casanovas (1975) with extrapolation from 11 to 14 $\text{kV} \cdot \text{mm}^{-1}$ and the filled circles are from the present investigation (Fig. 4) with extrapolation from 5.5 to 6.3 $\text{kV} \cdot \text{mm}^{-1}$.

t_{ref} =the reference temperature, (here 22°C) and k is the proportionality factor which depends on the electric field strength. The values of k are given in Table 1 and are compared with those from WICKMAN and CASANOVAS.

Initial recombination losses. The initial recombination, i.e. the recombination of ions formed in close proximity to one another, need generally not to be considered for gas-filled ionization chambers but is of great importance for a liquid chamber, due to the much higher density and considerably lower mobility of the ions of the sensitive detector material. The initial recombination per unit absorbed dose does not depend on the dose rate as it occurs within a single track but is affected by the temperature and the electric field strength. The number of ions formed close to one another increases with the LET, thus increasing the initial recombination.

The theory of JAFFE (1913) was utilized for determination of the initial recombination losses. The value of the inverse of the measured charge, $1/Q$, was plotted versus the inverse of the electric field strength over the liquid, $1/E$, the so-called Jaffe plot, for E between 2.0 and 6.3 $\text{kV} \cdot \text{mm}^{-1}$. Jaffe plots for 200 kV roentgen ray, ^{60}Co γ and electron beams are shown in Fig. 4. At sufficiently high electric field strengths the curves become almost linear. The highest value used, 6.3 $\text{kV} \cdot \text{mm}^{-1}$, is still somewhat low to allow accurate extrapolations. However, measurements above this electric field strength

were not possible as the leakage current increased rapidly. An extrapolation to infinite E was performed from the fairly linear part between 5.5 and 6.3 $\text{kV}\cdot\text{mm}^{-1}$ to determine the D_w/Q -axis intercept or the saturation charge Q_{sat} at a given absorbed dose. The ion escape probability or the collection efficiency $p=Q/Q_{\text{sat}}$, could then be determined (Fig. 5) for the different field strengths in a ^{60}Co γ beam and compared with similar measurements by CHU et coll. and CASANOVAS (1975). The large discrepancies between the results seem to be caused by the difference in the field strength intervals used for extrapolation. The collecting efficiency obtained in the present investigation still seems to overestimate the efficiency somewhat since the curve in the Jaffe plot has not completely reached the linear region. The high values by CHU et coll. should be expected as they used a field strength as low as 2.0 $\text{kV}\cdot\text{mm}^{-1}$ in the extrapolation procedure.

At a field strength of 6.0 $\text{kV}\cdot\text{mm}^{-1}$ the collection efficiency in the high energy electron beams was found to be a few per cent higher than in the ^{60}Co γ beam and it was as much as about 25 per cent lower for the roentgen ray. This difference should be expected as there are only small differences in mean LET for ^{60}Co γ and electron beams but conventional roentgen rays have a significantly larger LET.

Yield of ions. The response as a function of the electric field strength is shown for photon and electron beams in Fig. 3. The intercept $|E_{\text{ex}}|$, determined from extrapolation to the x-axis, is independent of the dose rate, provided corrections for general recombination have been carried out, but $|E_{\text{ex}}|$ has different values for different beam qualities. It has thus been shown that $|E_{\text{ex}}|$ decreases with mean LET (CASANOVAS). This is, however, not necessarily true for mixtures of high and low LET radiations (e.g. a beam mixed of photons and neutrons) as the response is considerably lower with high LET radiation due to the increased initial recombination. In a mixture of high and low LET radiation the signal is therefore mainly due to the low LET fraction (CHU et coll.). It is seen from Fig. 3 that $|E_{\text{ex}}|$ is somewhat lower for ^{60}Co γ beams than for electron radiation but considerably lower for conventional roentgen rays (200 kV). This variation is consistent with the differences in LET.

The free ion yield G_{fi} defined from the relationship

$$G_{\text{fi}}(E) = \frac{Q(E)}{mD_i} \quad (2)$$

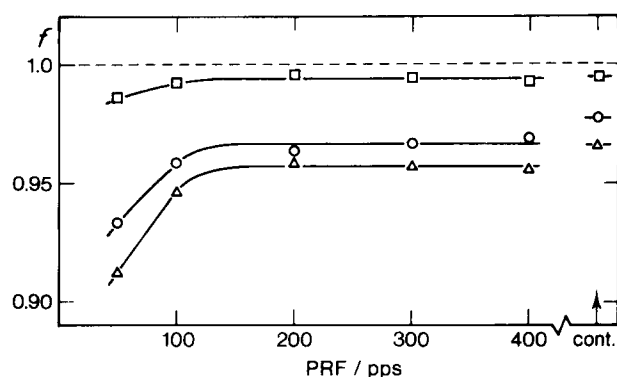


Fig. 6. The general collection efficiency, f , versus the pulse repetition frequency for electron beam with $E_0=11$ MeV and for continuous radiation (^{60}Co γ) are given. The dose-rates are 0.9 $\text{Gy}\cdot\text{min}^{-1}$ (\square), 3.8 $\text{Gy}\cdot\text{min}^{-1}$ (\circ) and 5.6 $\text{Gy}\cdot\text{min}^{-1}$ (\triangle).

Table 2

Yield of free ions, G_{fi} in $\text{C}\cdot\text{J}^{-1}$ at an electric field strength of 2.7 $\text{kV}\cdot\text{mm}^{-1}$ for different beam qualities. The uncertainties are mainly due to difficulties in determining the mass of the sensitive volume of the liquid

Quality	Present investigation	WICKMAN (1974)	CASANOVAS (1975)
200 kV roentgen ray	0.007±0.001		
^{137}Cs γ			0.0088
^{60}Co γ	0.012±0.001		0.0093
15 MeV electrons	0.013±0.001	0.0126	

Table 3

Empirical constants to be used for the calculation of recombination correction factors in eqs 4 a and 4 b for the liquid chamber described in Fig. 1

E ($\text{kV}\cdot\text{mm}^{-1}$)	$c_1/\text{min}\cdot\text{Gy}^{-1}$		c_2/Gy^{-1}
	^{60}Co gamma beams	Electron and photon beams (p.r.f. 150–400 s^{-1})	Electron and photon beams (p.r.f. ≤ 100 s^{-1})
1.5	0.0120	0.0160	0.10
2.7	0.0060	0.0080	0.050
4.7	0.0036	0.0048	0.030

has been investigated as a function of the electric field strength, E , by CASANOVAS for several types of liquids. Here $Q(E)$ is the collected charge of one sign at the reference temperature if the general recombination loss is assumed to be zero. m is the mass of the liquid in the sensitive volume at the reference temperature and D_i is the absorbed dose to the liquid determined according to the method

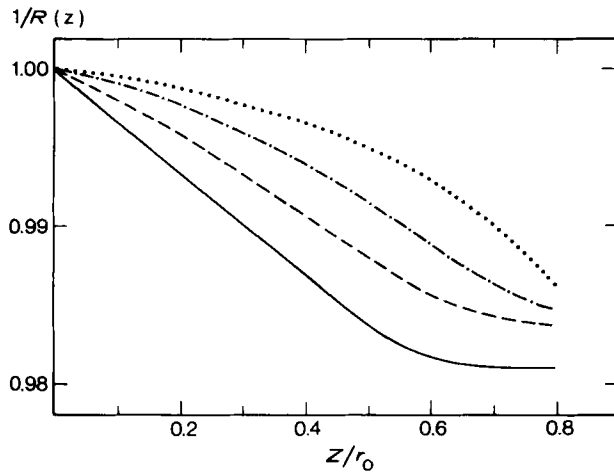


Fig. 7. The angle-dependent correction factor, $1/R(z)$, for the liquid chamber as a function of the depth, z , expressed as a fraction of C.S.D.A.-range, r_0 . The relation is given in eq. 8 and with $\epsilon=0.04$ and $\theta_0^2=0.76$. The energies of the electron beams at the surface of the phantom are, 5 MeV (—), 10 MeV (---), 20 MeV (- · -) and 40 MeV (···).

Table 4

Normalized readings given at different angles between the surface of the chamber and the direction of the beam. The field sizes are 10 cm × 10 cm and the depth for ^{60}Co γ beam is 10 cm and the depth for the electron beams is 2 cm

Angle (degrees)	Normalized readings		
	^{60}Co γ	Electron beams	
		$\bar{E}_0=19$ MeV	$\bar{E}_0=11$ MeV
0	1.000	1.000	1.000
15		1.006	0.997
30	1.002	1.012	1.001
45	1.012	1.023	1.007
90	1.040		

described on page 365. Also the G_{fi} value, for a given value of E , is strongly quality (LET) dependent as can be seen from measurements carried out in the present investigation and by WICKMAN and CASANOVAS (Table 2). The mean energy expended in the liquid per ion pair formed, W , is related to the $G_{\text{fi}}(E)$ through

$$\frac{W}{e} = \frac{p}{G_{\text{fi}}(E)} \quad (3)$$

The value of $G_{\text{fi}}(E)$ was determined to $(0.012 \pm 0.001) \text{ C} \cdot \text{J}^{-1}$ at $E=2.7 \text{ kV} \cdot \text{mm}^{-1}$ (Table 2). With p taken from CASANOVAS (cf. Fig. 5) this gives a W/e value for isoocetan of $(25 \pm 2) \text{ J} \cdot \text{C}^{-1}$

using ^{60}Co γ beam. This could be compared with published values between 22 and 43 $\text{J} \cdot \text{C}^{-1}$ (cf. CHU et coll.). The higher values could partly be explained by the relatively high p -values obtained at too low field strengths.

General recombination losses. The general recombination was experimentally determined by comparison with an air ionization chamber by varying the dose rate. The air-ionization chamber has a fairly small recombination loss and furthermore its numerical value is well known and was corrected for. Experiments were carried out both for continuous radiation (^{60}Co γ) and pulsed radiation of different pulse repetition frequencies (p.r.f.). The collection efficiency, f , was measured as a function of the p.r.f. at a constant mean dose rate (Fig. 6). It is seen that the efficiency is almost independent of the p.r.f. above about 150 s^{-1} . The reason for this is that when the transport time of the ions in the liquid is longer than the duration between two consecutive pulses the continuous irradiation case is approached with regard to the ion density in the liquid. The collection efficiency for such radiation gives the upper limit which has a dose rate dependence given by the expression

$$\frac{1}{f} = 1 + \bar{D} \cdot c_1 \quad (4a)$$

where \bar{D} is the mean dose rate in $\text{Gy} \cdot \text{min}^{-1}$ and $c_1=0.006 \text{ min} \cdot \text{Gy}^{-1}$ for continuous radiation and $c_1=0.008 \text{ min} \cdot \text{Gy}^{-1}$ for pulsed radiation at p.r.f. between about 150 and 400 s^{-1} with $E=2.7 \text{ kV} \cdot \text{mm}^{-1}$. The correction factor has been experimentally investigated for dose rates between 0.1 and $5.6 \text{ Gy} \cdot \text{min}^{-1}$. Values of c_1 , at other E -values are given in Table 3.

Below a p.r.f. of about 100 s^{-1} the collection efficiency for a certain mean absorbed dose rate decreases rapidly with a decrease in p.r.f., as the dose per pulse increases and the charge transport time is of the same order or shorter than the time between pulses. The recombination losses should therefore be dependent mainly on the absorbed dose per pulse assuming the pulse length to be much shorter than the charge transport time. An empirical relation for $1/f$ was obtained

$$\frac{1}{f} = 1 + D_p \cdot c_2 \quad (4b)$$

where D_p is the absorbed dose per pulse in mGy and c_2 is a constant that depends on the field strength.

The relation is valid for a p.r.f. below 100 pps and for D_p below about 5 mGy. Values for c_2 are given in Table 3.

A comparison with values based on the relationship by BOAG (1950) was made

$$\frac{1}{f} = \frac{u}{m(1+u)} \quad (5)$$

where

$$u = \frac{\alpha}{\mu} \frac{d^2 n(E)}{V} \quad (6)$$

μ is the mobility of ions, α is the recombination coefficient, d is the separation between the electrodes, and V is the potential. $n(E)$ is the number of ion pairs per volume in the liquid escaping initial recombination at the electric field strength of E and can be written

$$n(E) = D_p \rho G_{\text{fi}}(E) \quad (7)$$

The following numerical values were applied: $\alpha/\mu = 0.93 \cdot 10^{-6} \text{ V} \cdot \text{m}$ (from WICKMAN), $d = 0.32 \cdot 10^{-3} \text{ m}$, $V = 850 \text{ volt}$, $D_p = 1.0 \cdot 10^{-3} \text{ Gy}$, $\rho = 0.69 \cdot 10^{-3} \text{ kg} \cdot \text{m}^{-3}$ and $G_{\text{fi}}(E) = 0.013 \text{ C} \cdot \text{J}^{-1}$. These values give $1/f = 1.035$ to be compared with 1.05 using experimental data (eq. 4b). The theoretical value thus underestimates the recombination losses. The reason could be the values used for α/μ . Experimentally determined values for recombination losses are therefore recommended both for continuous and pulsed radiation.

Dependence on angle. Experiments were performed to determine the angular dependence of the chamber in electron and ^{60}Co γ beams. The response of the chamber was measured in a water phantom at different angles between the surface of the chamber relative to the direction of the incident beam (Table 4). The readings are normalized to the case where the front surface of the chamber is perpendicular to the direction of the beam, 0° . The response of the chamber increases with increasing inclination of the chamber. This means that the response can be expected to increase somewhat with depth in an electron beam as the angular distribution of the electron is broader at greater depths. The high value of 1.040 in a ^{60}Co γ beam with the surface parallel to the direction of the beam, 90° , could be due partly to interface phenomena and lower photon absorption in the low-density liquid.

The experimental data were fitted by an expression suggested by BRAHME (1982) in order to evalu-

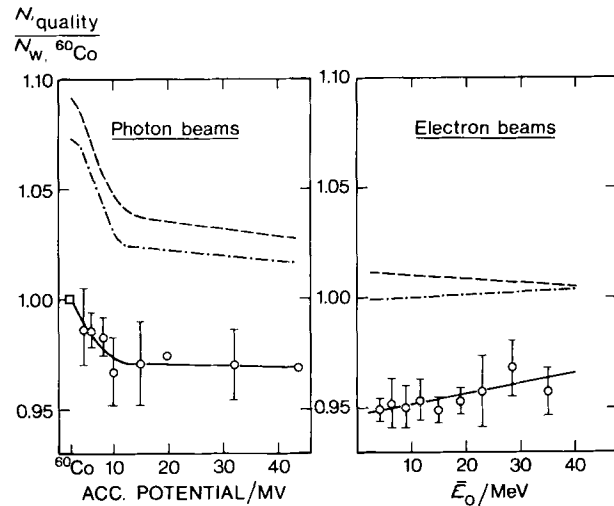


Fig. 8. The absorbed dose to water calibration factor, N_w (—), the absorbed dose to liquid calibration factor, N_D (---), and the absorbed dose to liquid calibration factor corrected for the angle dependence, N_D (---), as a function of the quality of the beam. All values are normalized to N_w for a ^{60}Co γ beam. The uncertainty given corresponds to the 95 per cent confidence level.

ate a correction factor, $1/R(z)$, which takes into account the angular dependence of the chamber. The dependence of the detector response on the angular spread is given by

$$R(z) = 1 + \varepsilon \frac{\bar{\theta}^2(z)}{\theta_d^2 + \bar{\theta}^2(z)} \quad (8)$$

where ε is the relative increase of the detector response from small (i.e. perpendicularly incidence on the chamber wall) to large angles of the incident particle. $\bar{\theta}^2(z)$ is the mean square angular spread of the electrons at the point of measurement at depth z and θ_d is a characteristic detector angle which describes how quickly the response varies. Fig. 7 shows the angular dependent correction factor, $1/R(z)$, as a function of depth in the phantom and energy at the phantom surface for electron beams. For the calculations of $1/R(z)$, the values given by BRAHME for the liquid chamber, $\varepsilon = 0.04$ and $\theta_d^2 = 0.76$ have been used. Similar calculations can be carried out for photon radiation (cf. BRAHME).

Clinical application

The use of the liquid chamber for absorbed dose determination in megavoltage photon and electron beams has been investigated. Measurements were carried out during the dosimetric intercomparison in

Table 5

Empirical quality factor, C_L , to be used for the calculation of the absorbed dose according to eq. 11. The factors are normalized at an energy \bar{E}_0 of 20 MeV

Quality	Depth (mm)	C_L
$^{60}\text{Co } \gamma$	50	1.045
6 MV rtg ray	50	1.03
10 MV rtg ray	100	1.02
20 MV rtg ray	100	1.015
30 MV rtg ray	100	1.015
40 MV rtg ray	100	1.01
5 MeV e^-	10	0.99
10 MeV e^-	20	0.995
20 MeV e^-	30	1.000
30 MeV e^-	30	1.005
40 MeV e^-	30	1.01

the Scandinavian countries (JOHANSSON et coll. 1982) at many different types of accelerators. The absorbed dose to water, D_w , at the reference point was determined using an air ionization chamber according to the procedure recommended in NACP (1980, 1981). The liquid ionization chamber was placed at a position in the water phantom where D_w had been determined for a given monitor reading. Four different liquid chambers were used in the investigation. The reading on the electrometer was corrected for temperature and general recombination losses, Q_{corr} , according to eqs 1, 4a and 4b. The absorbed dose to water calibration factor, N_w , is given by the relation $N_w = D_w / Q_{\text{corr}}$. The N_w values for all qualities were normalized to $^{60}\text{Co } \gamma$ beam values.

Electrons beams. The values of N_w determined at the reference depth for electron beams with mean energies at the phantom surface are shown in Fig. 8. The value of N_w is weakly dependent on the electron energy. In order to take into consideration the variation of the response with the angular distribution and the difference in stopping power between water and the detector liquid an absorbed dose to the detector liquid calibration factor, N_D , was calculated.

$$N_D = N_w R(z) s_{1,w} \quad (9)$$

where $s_{1,w}$ is the collision mass stopping power ratio 2,2,4-trimethylpentane to water. For the calculation of $R(z)$ (eq. 8) it was assumed that the beam is plane-parallel at the phantom surface. In real clinical beams there is an angle distribution already at the

surface of the phantom, which decreases the variation of $R(z)$ with depth. N_D will be almost quality independent in the energy range of the electron beam from 4 to 40 MeV (Fig. 8). The variation of N_D with radiation quality is in reality much smaller than the uncertainty in the quality dependence of stopping power ratios and perturbation correction factors used for determination of absorbed dose with an air-ionization chamber. The correction for the angular distribution may be disregarded at the reference depth for most practical purposes ($R(z)=1.0$); the calibration factor N_D' is then obtained. A set of measurements for N_w as a function of the phantom depth were performed. Also in this case a straight line is obtained provided correction for angular dependence $R(z)$ is applied.

Photon beams. The values of N_w obtained for photon beams with quality $^{60}\text{Co } \gamma$ to 45 MV roentgen rays are shown in Fig. 8. The change in the value is fairly rapid at qualities below 10 MV roentgen rays. The absorbed dose to the detector liquid calibration factor (not corrected for angular distribution) N_D' is also calculated for photon beams. The relation between N_D' and N_w is given by relation

$$N_D' = N_w F_{1,w} \quad (10)$$

where $F_{1,w}$ is the ratio of absorbed dose to liquid and absorbed dose to water. In order to calculate $F_{1,w}$ general cavity theory (BURLIN 1966) was applied as some of the electrons contributing to the absorbed dose in the liquid are generated in the phantom and some in the liquid itself. The ratio of the thickness of the liquid cavity in the direction of the beam to the mean CSDA-range for the electrons has been used in order to estimate the fraction of electrons generated in the liquid. This showed that about 15 per cent of the electrons in a $^{60}\text{Co } \gamma$ beam are generated in the liquid and about 1 per cent for 40 MV roentgen rays. The N_D' values calculated in this way are given in Fig. 8. There is still a relatively large change in N_D' below 10 MV roentgen rays. A minor part of this change may be explained from the fact that some electrons are generated in the front wall (0.3 mm Rexolite) and the watertight PMMA wall (1 mm). The major part must, however, be due to other reasons. The rapid change of $G_{\text{fl}}(E)$ with beam quality seems to be the main reason.

Correction of N_D' due to the broad angular distribution of the photon generated electrons further increase the response difference for high energy

photon compared with electron beams. The corrected values, N_D , are also shown in the figure.

Procedure for absorbed dose determination. The liquid chamber is very useful and suitable for absorbed dose determination, particularly in electron beams. However, in photon beams the chamber can also be used if correction for the quality dependence is carried out. In order to use the liquid chamber for absorbed dose determinations it is necessary to know the absorbed dose to water calibration factor, N_w , for the chamber. It is recommended that N_w is determined in an electron beam of approximately 20 MeV. The absorbed dose to the reference point in water for a given monitor reading should be determined by an air ionization chamber or by another accurate method. The liquid ionization chamber should be placed at the same reference point. The measured charge from the liquid chamber must be corrected for temperature and general recombination losses, Q_{corr} , and the absorbed dose to water calibration factor, N_w , for the quality used is then given by D_w/Q_{corr} . For measurements at other qualities the simplest way to determine the absorbed dose to water for that quality is to use a correction factor, C_L , that takes into account the LET- and angular-dependence and also corrects for the ratio absorbed dose water to liquid for both the calibration and quality used.

The absorbed dose at other qualities than the calibration quality is then given by

$$D_w = N_w \cdot Q_{\text{corr}} \cdot C_L \quad (11)$$

Values for the quality dependent factor, C_L , normalized to measurements in a beam with \bar{E}_0 between 16 and 24 MeV are given in Table 5. This energy region was chosen as it is possible to make calibrations against a thimble ionization chamber with an acceptable uncertainty due to the small perturbation correction (MATTSSON et coll.). These are also the maximum energies obtained with many electron accelerators. The values are experimentally determined (from Fig. 8) and are valid at an electric field strength of about $2.7 \text{ kV} \cdot \text{mm}^{-1}$. The variation of C_L would decrease slightly with an increase in the field strength.

Conclusion

The use of the liquid ionization chamber for dosimetry of electron and photon beams in the megavolt-

age range has been investigated. The chamber is particularly suitable for absorbed dose determination in electron beams since the relation between measured charge and absorbed dose to water is almost energy independent. This is due to the small variation of the collision mass stopping power ratio, water to the liquid for electrons between 0.1 and 50 MeV. The variation is only 3 per cent, while the water to air ratio varies by about 25 per cent. For absorbed dose determination in the reference point a convenient procedure is therefore to calibrate the chamber for one electron beam quality and use it for absorbed dose determination in other electron beams. For photon beams the determination is somewhat more complicated due to the change in the relation between measured charge and absorbed dose to liquid particularly at photon beams with the quality below 10 MV. The change in response is most probably due to the change in the yield of free ions per absorbed dose. However, correction factors are given for this change in response and the liquid chamber can thus be used for absorbed dose determinations in photon beams when the calibration has been carried out in an electron beam.

The reproducibility of the measurements and the long-time stability are almost as good as for an air-filled ionization chamber even when the chamber has been refilled with liquid between the measurements. The leakage current is low and always less than one per cent of the ionization current even in radiation therapy fields with low dose rates. Corrections for temperature dependence and general recombination losses must generally be applied. The yield of free ions, the initial recombination losses and the mean energy expended in the liquid per ion pair formed have been experimentally investigated. The yield of free ions is very sensitive to changes in LET. In a ^{60}Co γ beam the yield of free ions is 6 per cent lower than in an electron beam with an energy of 20 MeV assuming an electric field strength E of $2.7 \text{ kV} \cdot \text{mm}^{-1}$ is used which is a suitable value for practical reasons. The technique for carrying out the practical measurement is not more complicated than for an air-ionization chamber. Also the handling of the chamber is fairly simple using the technique described. It is the authors' opinion that this chamber should be very suitable for absorbed dose determination in electron and photon beams and should in many cases replace the air-ionization chamber particularly when the uncertainties in $s_{w,\text{air}}$ and perturbation correction may be large.

SUMMARY

The use of a liquid ionization chamber for measurements in electron and photon beams with energies above 1 MeV has been investigated. The liquid in the chamber is 2,2,4-trimethylpentane. Fundamental properties such as the reproducibility of the measured charge per absorbed dose, the temperature dependence, and the angular dependence have been experimentally analysed. The general recombination losses in pulsed beams are shown to be dependent on the transport time of the ions in the liquid. For a longer transport time than the time between two consecutive pulses the losses depend on the mean dose rate and for a shorter transport time the losses depend on the absorbed dose per pulse. The Jaffe method is used for determination of the initial recombination losses, and compared with results from other authors. The chamber is particularly useful for absorbed dose determination in electron beams since the relation between measured charge and absorbed dose to water is almost energy independent. In photon beams the relation is somewhat quality dependent particularly at qualities below 10 MV. The change of the free ion yield caused by the small change of mean LET with the quality of the photon beam is probably the reason. Procedures for the calibration of the liquid chamber and the absorbed dose determination in electron and photon beams are described.

ACKNOWLEDGEMENTS

The authors would like to thank Thord Holmström for the technical work on the chambers used. Useful comments have been given by Anders Brahme, Lars-Olof Mattsson and Alan Nahum.

REFERENCES

- BOAG J. W.: Ionization measurements at very high intensities. *Brit. J. Radiol.* 23 (1950), 601.
- BRAHME A.: Correction for the angular dependence of a detector in electron and photon beams. *Acta radiol. Oncology* 21 (1982).
- BURLIN T. E.: A general theory of cavity ionization. *Brit. J. Radiol.* 39 (1966), 727.
- CHU J. C. H., GRANT III W. H. and ALMOND P. R.: A liquid ionization chamber for neutron dosimetry. *Phys. Med. Biol.* 25 (1980), 1133.
- CASANOVAS J.: Etude de la conduction induite par des rayonnements à transferts linéiques d'énergie très différent dans certains liquides organiques non polaires. Thesis, Université Paul Sabatier, Toulouse, 1975.
- JAFFE G.: Zur Theorie der Ionisation in Kolonnen. *I. Ann. Physik* 42 (1913), 303.
- JOHANSSON K.-A., MATTSSON L. O. and SVENSSON H.: Dosimetric intercomparison at the Scandinavian radiation therapy centres. I. Absorbed dose intercomparison. *Acta radiol. Oncology.* 21 (1982), 1.
- MATHIEU J.: Thèse d'Etat ès Sciences Physique, n° 113, Toulouse 1968.
- MATTSSON L. O., JOHANSSON K.-A. and SVENSSON H.: Calibration and use of plane-parallel ionization chambers for the determination of absorbed dose in electron beams. *Acta radiol. Oncology* 20 (1981), 385.
- NORDIC ASSOCIATION OF CLINICAL PHYSICS (NACP): Procedures in external radiation therapy dosimetry with electron and photon beams with maximum energies between 1 and 50 MeV. *Acta radiol. Oncology* 19 (1980), 55.
- Electron beams with mean energies at the phantom surface below 15 MeV. Supplement to the recommendations by NACP (1980). *Acta radiol. Oncology* 20 (1981), 401.
- WICKMAN G.: A liquid ionization chamber with high spatial resolution. *Phys. Med. Biol.* 19 (1974), 66.